

Depth-Dependent Transverse Shear Properties of the Human Corneal Stroma

Steven J. Petsche,¹ Dimitri Chernyak,² Jaime Martiz,³ Marc E. Levenston,¹ and Peter M. Pinsky¹

PURPOSE. To measure the transverse shear modulus of the human corneal stroma and its profile through the depth by mechanical testing, and to assess the validity of the hypothesis that the shear modulus will be greater in the anterior third due to increased interweaving of lamellae.

METHODS. Torsional rheometry was used to measure the transverse shear properties of 6 mm diameter buttons of matched human cadaver cornea pairs. One cornea from each pair was cut into thirds through the thickness with a femtosecond laser and each stromal third was tested individually. The remaining intact corneas were tested to measure full stroma shear modulus. The shear modulus from a 1% shear strain oscillatory test was measured at various levels of axial compression for all samples.

RESULTS. After controlling for axial compression, the transverse shear moduli of isolated anterior layers were significantly higher than central and posterior layers. Mean modulus values at 0% axial strain were 7.71 ± 6.34 kPa in the anterior, 1.99 ± 0.45 kPa in the center, 1.31 ± 1.01 kPa in the posterior, and 9.48 ± 2.92 kPa for full thickness samples. A mean equilibrium compressive modulus of 38.7 ± 8.6 kPa at 0% axial strain was calculated from axial compression measured during the shear tests.

CONCLUSIONS. Transverse shear moduli are two to three orders of magnitude lower than tensile moduli reported in the literature. The profile of shear moduli through the depth displayed a significant increase from posterior to anterior. This gradient supports the hypothesis and corresponds to the gradient of interwoven lamellae seen in imaging of stromal cross-sections. (*Invest Ophthalmol Vis Sci.* 2012;53:873–880) DOI:10.1167/iovs.11-8611

From the ¹Department of Mechanical Engineering, Stanford University, Stanford, California; ²Abbott Medical Optics, Inc., Milpitas, California; and ³International Refractive Consultants, LLC, Houston, Texas.

Supported by National Institutes of Health Grant R01AR052861 (MEL), Stanford University Bio-X Interdisciplinary Initiatives Program (PMP), and Stanford Graduate Fellowship (SJP).

Submitted for publication September 16, 2011; revised December 2, 2011; accepted December 11, 2011.

Disclosure: **S.J. Petsche**, None; **D. Chernyak**, Abbott Medical Optics, Inc. (E); **J. Martiz**, International Refractive Consultants, LLC (E); **M.E. Levenston**, None; **P.M. Pinsky**, None

Presented in part at the annual meeting of the Association for Research in Vision and Ophthalmology, Fort Lauderdale, Florida, May 2011, and the American Society of Mechanical Engineers 2010 Summer Bioengineering Conference, Naples, Florida, June 2010.

Corresponding author: Peter M. Pinsky, 221 Durand Building, 496 Lomita Mall, Stanford University, Stanford, CA 94305-4040; pinsky@stanford.edu.

Thorough characterization of the mechanical properties of connective tissue, including the cornea, presents significant theoretical and experimental challenges. To date, mechanical testing of the cornea has been almost exclusively focused on estimating the tensile modulus of the stroma using techniques such as strip tensile tests or cornea pressure-inflation tests.^{1–4} However, even in the most simple of material models there are at a minimum two elastic constants that must be measured to characterize the three-dimensional elastic behavior of the material. This most simple case is called isotropic elasticity⁵ and occurs when the material properties under investigation exhibit no dependence on direction during testing. In this case, the material is fully characterized by the Young's modulus and the shear modulus. The shear modulus naturally measures the resistance of the tissue to shearing strains. In fact, the microstructure of the corneal stroma suggests that its elasticity cannot be isotropic. The parallel arrays of collagen fibrils within each lamella and the layering of lamellae one on another imply that the transverse (anterior-posterior) properties of the tissue will be different from the in-plane properties. To address this anisotropy and other considerations, increasingly complex elasticity models have been introduced with the goal of achieving greater fidelity to the full three-dimensional behavior of the tissue.^{6–8} More complex models always have more than two intrinsic elastic constants that need to be measured. When such models are extended to nonlinear behavior, yet more constants must necessarily be introduced (Petsche SJ, et al., manuscript submitted, 2012).^{6,8}

Experimental measurement of elastic constants must be interpreted against an assumed elasticity model (i.e., material symmetry). Transversely isotropic linear elasticity⁵ is the simplest possible model that can reasonably be applied to the corneal stroma. Materials exhibiting transverse isotropy have a single plane of material isotropy (the corneal tangent plane) and properties in this plane will be different from properties measured orthogonally (through the corneal thickness). In this case, characterization of the material elasticity requires the measurement of five independent elastic constants: the in-plane Young's modulus (related to the tensile modulus) and transverse Young's modulus, the in-plane and transverse Poisson's ratios, and the transverse shear modulus, denoted G .⁵ To appreciate the role of the transverse shear modulus, consider the anterior and posterior surfaces of a circular stromal button subjected to relative torsional twisting about an axis perpendicular to the surfaces (see Fig. 4). The tissue will become deformed in a state of pure transverse shear strain and the resistance of the tissue will be dependent only on the transverse shear modulus G . Experimental measurement of the shear properties of human corneas are missing from the extant literature. A thesis by Nickerson⁹ discusses the use of torsional rheometry to measure shear properties of porcine cornea. Standard inflation and strip testing^{1–4} do not introduce shearing deformations and these tests therefore give no information about shear stiffness.

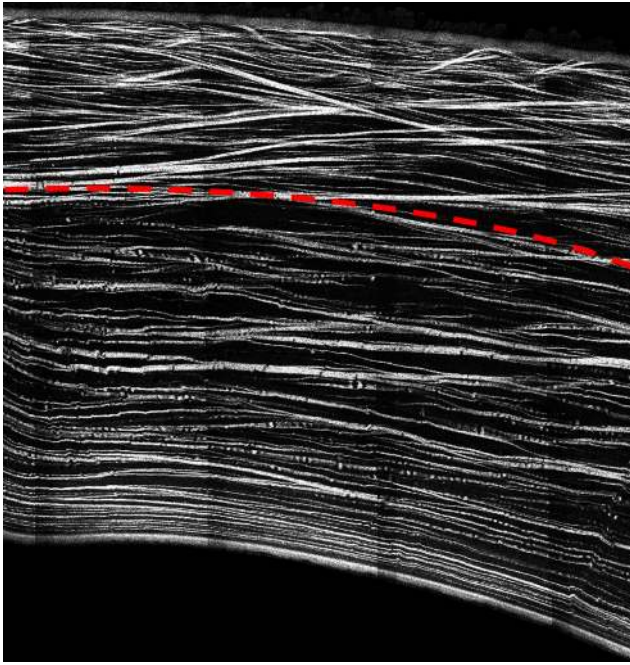


FIGURE 1. Cross-section of a human cornea from second harmonic generated imaging showing the interweaving of lamellae in the anterior third.

Because the corneal stroma makes up 90% of the tissue's thickness and contains almost all the cornea's collagen and proteoglycan content, it is the crucial layer for explaining corneal stiffness. The stroma consists of 200 to 500 sheet-like lamellae, each made up of collagen fibrils maintained at quasi-uniform spacing for transparency by the glycosaminoglycan (GAG) chains of the stromal proteoglycans. Evidence of lamellar interweaving that varies with depth through the cornea is provided by imaging that uses polarized light.¹⁰ The interweaving appears maximal at the anterior surface and significantly reduces toward the posterior. Recent images by Jester et al.^{11,12} using second harmonic generated imaging confirm this assessment. Figure 1 shows the central part of a full human cornea cross-section created from many second harmonic generated images and in which distinct interweaving in the anterior third may be discerned by the through-thickness trajectory of many of the lamellae. It is also noted that scanning electron microscopy and transmission electron microscopy images show that lamellae become wider and thicker toward the posterior of the stroma.¹³ X-ray scattering studies have demonstrated that the collagen associated with preferred directions measured in the limbal plane also varies with depth through the cornea.¹⁴ After using a femtosecond laser to cut the stroma into thirds through the thickness, Abahussin et al.¹⁴ showed that lamellae exhibit preferred angular distributions in the posterior third but transition toward a more uniform distribution in the anterior third.

The complex patterns of the three-dimensional collagen architecture within the stroma can be expected to affect and

contribute to the elasticity of the tissue regionally. In particular, the variation of microstructure through the thickness suggests that the mechanical properties of the stroma may have a nonconstant profile through the thickness. Depth dependence of mechanical properties in the stroma, including transverse shear stiffness, has not been considered heretofore and may be important for the biomechanics of the cornea. We hypothesize that the pronounced interweaving of lamellae in the anterior third compared with the central and posterior thirds will provide the anterior third with a relatively larger transverse shear modulus because the collagen in vertically descending lamellae may be engaged during the shearing deformations. This will not be the case in noninterweaving regions. In this work we report direct measurement of the transverse shear modulus of the human corneal stroma through the depth using torsional rheometry.

METHODS

Sample Preparation

Four matched human cornea pairs (donor ages 82–86) were obtained from the San Diego Eyebank either 1 week (Donor 1 and 2) or 2 weeks (Donor 3 and 4) postmortem. Handling and experimental protocol adhered to the tenets of the Declaration of Helsinki. All samples were kept refrigerated at 5°C in corneal storage medium (Optisol; Bausch & Lomb, Irvine, CA) until testing to preserve the tissue.¹⁵ On acquisition, the central corneal thickness (CCT) of each cornea was measured with a pachymeter (IOPac, Reichert Inc., Depew, NY). The right cornea from each donor pair was mounted in an artificial anterior chamber (Barron; Katena Products, Inc., Denville, NJ) and divided into three layers through the thickness (Fig. 2a) with lamellar cuts from a femtosecond laser (IFS; Abbott Medical Optics, Inc., Santa Ana, CA). The left donor corneas were left intact and maintained in corneal storage medium (Optisol; Bausch & Lomb). To minimize swelling, the epithelium and endothelium were not removed until immediately before mechanical testing.¹⁶

The target stromal layer thickness for each cut cornea was calculated by subtracting the epithelial and endothelial thicknesses (assumed to be 53 μm ¹⁷ and 25 μm ¹⁸, respectively) from the CCT measurement and dividing by three. The thicknesses of Bowman's layer and Descemet's membrane were neglected in this calculation. Therefore, the first (posterior) laser cut was set at a depth equal to the stromal thickness plus the epithelium thickness beneath the anterior surface, while the second (central) and third (anterior) laser cuts were one and two stromal third thicknesses shallower, respectively. These three cuts were performed with an 8.5-mm diameter raster area, and a final 8 mm diameter, full thickness circular cut was made perpendicular to the other cuts. The raster pattern of the laser left some residual tissue bridging across the cutting plane which allowed each cornea to remain in one piece when placed back into corneal storage medium (Optisol; Bausch & Lomb) after the cuts.

All samples were tested within 56 hours of the laser cuts and were stored in corneal storage medium (Optisol; Bausch & Lomb) at 5°C until final preparation. Immediately before mechanical testing commenced, the epithelium and endothelium were removed by firmly wiping them off with a cleaning tissue (Kimwipe; Kimberly-Clark Corporation, Irving, TX). Each cut cornea was mounted in an artificial

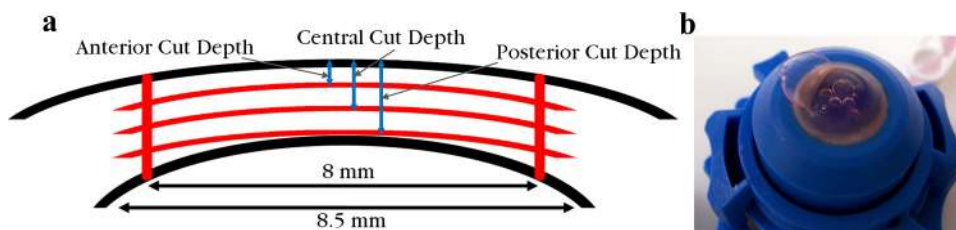


FIGURE 2. Four cuts were made with the femtosecond laser, three 8-mm diameter raster cuts at different depths and one 8.5-mm diameter circular cut through the thickness (a). An anterior third is shown in the process of separation immediately before testing (b).

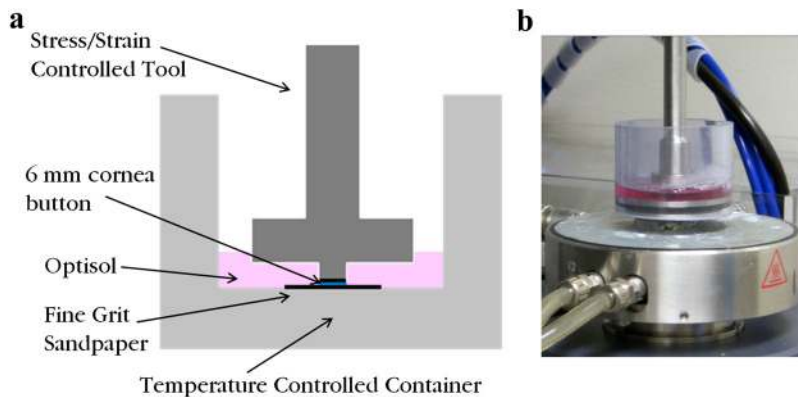


FIGURE 3. A schematic of the experimental setup indicates the position of the upper tool when the corneal button is tested in the torsional rheometer (a). The corneal storage medium (Optisol; Bausch & Lomb) bath was added after the upper tool had been lowered to the desired gap height for the first test. The photograph of the experimental setup shows the heating plate below the sample that keeps the bath at 37°C (b).

anterior chamber (Barron; Katena Products, Inc.), and the laser cut layers of the left corneas were separated with a spatula and forceps (Fig. 2b). The samples from each donor pair, consisting of three separated layers of the right cornea and the intact left cornea, were trimmed to a 6 mm diameter button with a biopsy punch. Forceps were used to grip the tissue only on the edge of the 8 mm diameter layers to avoid damaging the 6 mm diameter testing specimen.

Mechanical Testing

The transverse shear modulus of each sample at varying levels of axial compressive strain was measured with a torsional rheometer (AR 2000ex, TA Instruments, New Castle, DE). The 6 mm diameter buttons were gripped in the rheometer by applying axial compression with fine 320 grit sandpaper on both the top and bottom surfaces. A schematic and photograph of the testing apparatus are included in Figure 3. A force transducer recorded axial force applied during each torsion test.

The levels of applied axial strain for the torsion tests were different for full thickness and isolated layer samples because full thickness samples displayed more swelling. The initial compression for the isolated layer samples was applied by setting the gap distance with

micron precision to 10% more than the calculated stromal third thickness. Swelling immediately before testing allowed the tools to grip the tissue even with this expansive (positive) nominal strain. After gripping, a corneal storage medium (Optisol; Bausch & Lomb) bath was added and warmed to 37°C before the test. The first oscillatory shear test was performed at a frequency of 0.03 Hz and consisted of cyclic loading between -1% and 1% maximum shear strain (at the radial surface). Stress-strain data were recorded from the final cycle after approximately three cycles of preconditioning. The magnitude of the complex shear modulus (often denoted as G^*) was calculated from this stress-strain data. A typical stress-strain curve is shown in Figure 4. For the next oscillatory shear tests, axial compression was increased in 5% axial strain increments from 10% to -30% strain for every isolated layer sample except for one anterior sample where 10% increments were used. Compression was increased at a rate of 1 μ m per second followed by 3 minutes of stress relaxation time, based on stress relaxation curves from preliminary tests.

For the full thickness samples, the initial gap distance was set to be approximately 15% less than a CCT measurement taken immediately before gripping with a contact-sensing micrometer. This small increase of compressive strain allowed axial compressive stress to equilibrate by decreasing to a steady state in less than 5 minutes. After the initial compressive stress equilibrium was reached, an oscillatory shear test was performed as described above for the isolated layer samples. The gap distance was decreased in eight increments each 5% of the initial gap distance with the same rate and relaxation time used for the isolated layer samples. An identical oscillatory test was performed after every step of axial compression. The original CCT measurement minus assumed epithelium and endothelium thicknesses was used as the reference thickness and the gap distance as the current thickness for the axial strain calculation during each test.

The equilibrium axial compressive stress at a given axial strain was calculated as the axial force recorded during the oscillatory test divided by the initial cross-sectional area. This stress corresponds to the swelling pressure as defined in the cornea literature. Olsen and Sperling¹⁹ found a linear relationship between human corneal swelling pressure

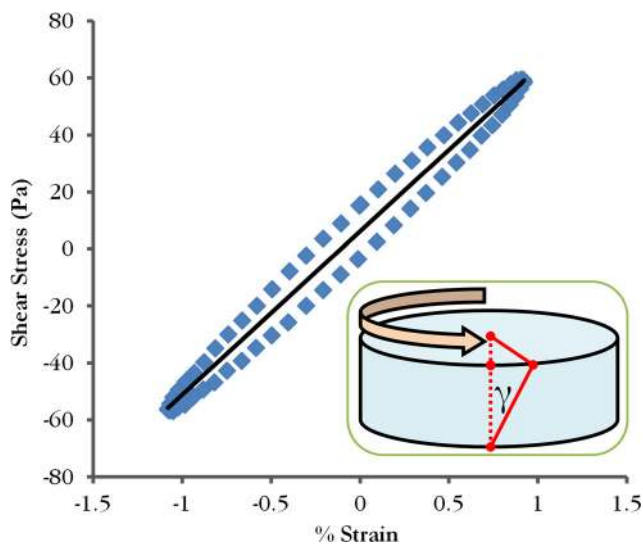


FIGURE 4. Typical stress/strain curve from a final load cycle used for calculating the magnitude of the complex shear modulus. The inset cartoon shows the applied torque and resulting shear strain (γ) on a cornea button, which is maximum at the perimeter.

TABLE 1. Measured Central Corneal Thickness Values for All Samples

Donor	CCT Uncut (Left)	CCT Cut (Right)	Stromal Third Thickness
1	550	600	174
2	525	530	150
3	575	625	182
4	654	650	190

Data shown are μ m.

TABLE 2. Mean Shear Modulus Values at 0% Axial Strain

Third Type	Anterior	Central	Posterior	Full
Mean	7.71	1.99	1.31	9.48
SD	6.34	0.45	1.01	2.92

Data shown are kPa.

and sample thickness when plotted on a double logarithmic scale. Therefore, their data were fit to a power equation of the form $SP = aT^b$, where SP is swelling pressure, T is sample thickness, and a and b are constants. Sample thickness can be related to axial strain with the equation $T = T_0(1 + \epsilon)$, where T_0 is the reference thickness and ϵ is the axial strain. Combining these equations gives a relationship between swelling pressure and axial strain: $SP = a[T_0(1 + \epsilon)]^b$. The derivative of equilibrium axial compressive stress (swelling pressure) with respect to strain gives the negative of the equilibrium compressive modulus as a function of strain. For each sample, equilibrium axial stress-strain data were fit to the above equation with the reference thickness taken as the same value used to calculate axial strain. The compressive modulus at 0% strain was then calculated from the derivative of the resulting fit equation.

Data Analysis

Data are presented as mean \pm SD. Significance was at $P < 0.05$. Initial CCTs of right and left corneas were compared using a paired t -test.

Axial strain was chosen as a covariate in the statistical analysis. Software (Minitab¹⁶; Minitab Inc., State College, PA) was used to perform an analysis of covariance (ANCOVA) on the log transformed shear modulus data with layer (anterior, central, and posterior) as a fixed factor and donor as a random factor. The shear modulus data were log transformed to achieve a homogeneous variance. Bonferroni pairwise comparison tests were used to compare third types.

An ANOVA was performed on equilibrium compressive modulus data with sample type (full, anterior, central, and posterior) as a fixed factor and donor as a random factor. Bonferroni pairwise comparison tests were used to compare sample types.

RESULTS

The CCTs of the corneas when received from the eye bank ranged from 525 μ m to 654 μ m ($589 \pm 52 \mu$ m, Table 1), and did not significantly differ between right and left corneas ($P = 0.17$). The targeted stromal third thicknesses used to define the depths of the laser cuts thus ranged from 150 μ m to 190 μ m.

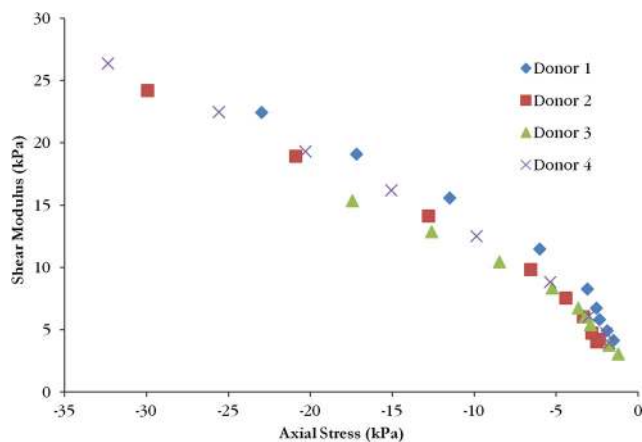


FIGURE 5. The shear moduli as a function of axial compressive stress for the full thickness samples from each donor displays a nonlinear relationship.

The shear moduli increased with increasing axial compressive strain for all samples. Values for full thickness corneas lay in the range of 3.06–26.38 kPa. Linear interpolation was used to calculate the mean shear modulus at 0% axial strain (Table 2). When plotted as a function of measured axial compressive stress, full thickness shear moduli curves from different donors show good agreement and follow a nonlinear relationship (Fig. 5). Anterior layer shear modulus values ranged from 1.7 to 25.6 kPa, central third values ranged from 0.88 to 7.15 kPa, and posterior third values ranged from 0.22 to 6.26 kPa. Shear modulus values as a function of axial strain are grouped by sample type in Figure 6 and by donor in Figure 7. Curves for the central layer fall between the curves for the anterior and posterior layers in three of the four donors. Average values of shear modulus values for each layer at 0% axial strain are found in Table 2. For the isolated layer samples, there was a significant effect of layer type on the shear modulus after accounting for the effect of axial strain ($P < 0.001$) and donor variability ($P = 0.033$). Anterior samples were stiffer than central samples ($P < 0.0001$) and central samples were stiffer than posterior samples ($P < 0.0001$).

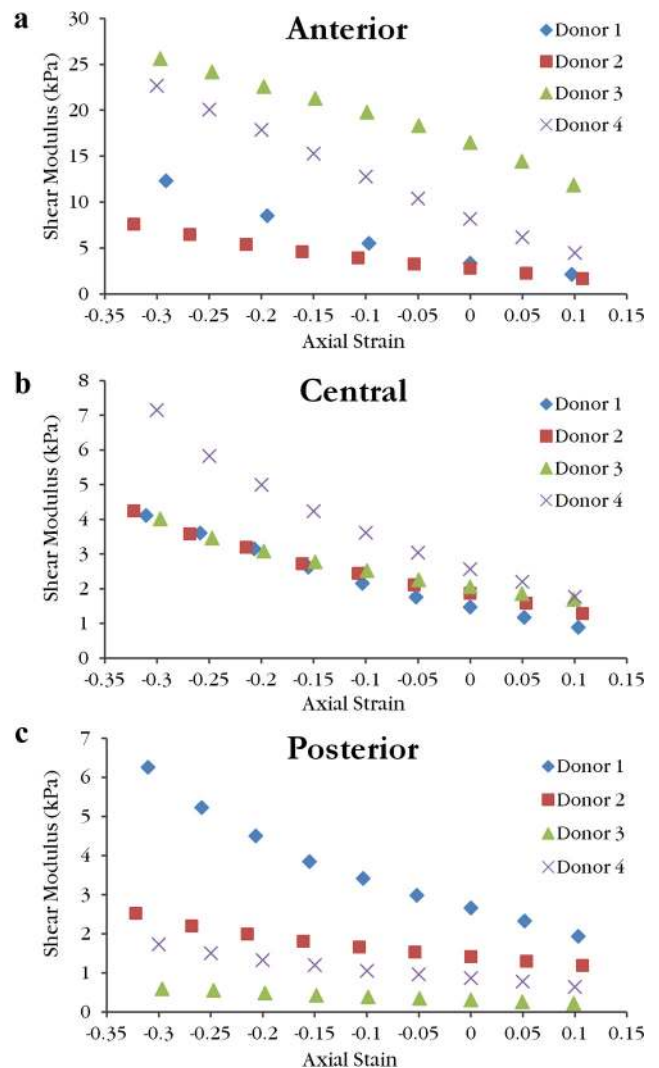


FIGURE 6. The shear moduli as a function of axial strain for the anterior (a), central (b), and posterior (c) isolated layer samples reveal the variation of moduli range between layers. Note the scale of the ordinate axis is larger for anterior samples when compared with central and posterior samples.

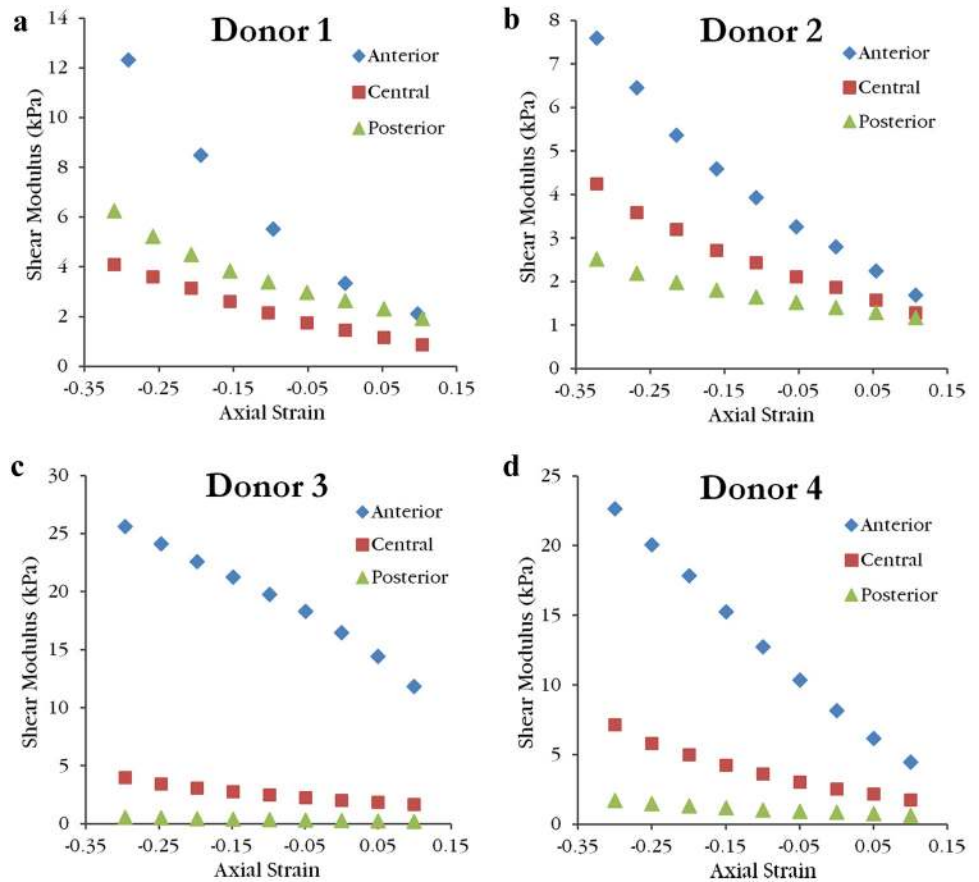


FIGURE 7. The shear moduli as a function of axial strain for the laser cut corneas from Donor 1 (a), Donor 2 (b), Donor 3 (c), and Donor 4 (d) illustrate that the anterior layer was stiffer than the central and posterior layers at all compressive strains. Also, except for Donor 1, the central layer was stiffer than the posterior layer at every compressive strain.

Qualitative comparison of full samples with the isolated layer samples from the same donor's contralateral cornea yielded different conclusions depending on whether the measured moduli were viewed as a function of axial strain or measured axial stress (Fig. 8). While the axial stress range of each sample varied, in areas where the stress ranges overlapped the full sample modulus was in between the anterior and central layer moduli from the same donor for a given axial stress.

Equilibrium axial compressive stress values as a function of axial strain are grouped by sample type in Figure 9. Equilibrium compressive moduli at 0% axial strain and the R^2 value of the power fit used to calculate each modulus are collected in Table 3. For 15 of the 16 samples, the power fit produced an R^2 value greater than 0.94 with nine samples greater than 0.99. Compressive moduli spanned a wide range from 0.79 to 49 kPa. The average full thickness sample compressive modulus of 38.7 ± 8.6 kPa matches well with the compressive modulus of 38.2 kPa calculated at normal thickness from the average power fit reported by Olsen and Sperling¹⁹ based on 45 human corneas. Sample type had a significant effect on equilibrium compressive modulus ($P < 0.001$) while donor did not show a significant effect ($P = 0.425$). Full samples were stiffer than all isolated layers ($P < 0.001$) but there were no significant differences among isolated layers ($P > 0.999$).

DISCUSSION

Shear properties of the cornea are important for understanding and modeling the mechanics of the tissue. The present study reports the transverse shear modulus of the human corneal stroma and characterizes the profile of the shear modulus through the depth. After controlling for axial strain, the ante-

rior layer samples were significantly stiffer than the central and posterior layer samples, as hypothesized. Close examination of results for each donor in Figure 7 reveals that, for a given compressive axial strain, the anterior layer modulus is two to five times greater than the central layer modulus, whereas the central and posterior layers are comparable. This trend matches the degree of lamellar interweaving seen in each third thickness of Figure 1. The anterior third thickness shows many lamellae that run transversely to the tangent plane. The collagen fibrils that make up each lamella have high tensile stiffness and interwoven lamellae would be stretched in transverse shear deformation thereby engaging the fibrils in shear resistance. In the posterior third thickness, lamellae remain mostly parallel to the tangent plane and therefore would not be stretched during shearing deformation. More interweaving, with corresponding fibril engagement resisting the deformation, will imply a higher shear modulus. This could explain the larger moduli in the anterior layer samples. Average shear modulus values for each layer at the estimated physiological thickness provide an immediate starting point for choosing shear properties of a computational model where shear stiffness can vary with depth in the stroma (Table 2).

Equilibrium axial compressive stress showed a power law relationship with axial strain, consistent with the findings of Olsen and Sperling.¹⁹ Measured swelling pressure values for full thickness samples were generally lower than the mean relationship reported by Olsen and Sperling (Fig. 9a). This is expected due to the different bath used during the tests. Optisol (Bausch & Lomb) contains dextran and chondroitin sulfate to help prevent swelling during storage which would lower swelling pressure.²⁰ Despite the lower swelling pressure values, the modulus values calculated at 0% axial strain for full thickness samples match well with the value calculated from

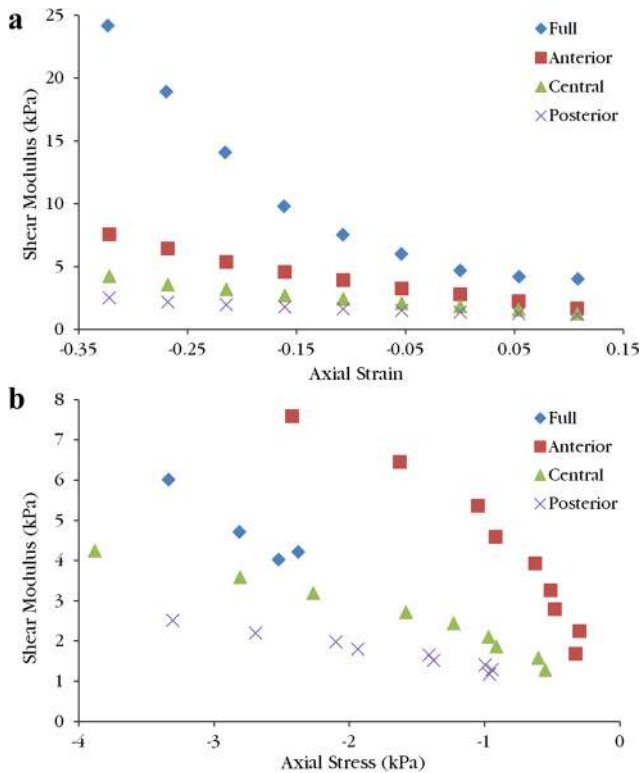


FIGURE 8. All shear moduli from Donor 2 are plotted as a function of axial strain (a) and axial compressive stress (b). The full thickness sample is stiffer than the isolated layer samples for a given axial strain. Full sample modulus values fall between the anterior and central samples at a given axial stress. On both graphs, moving left corresponds to increasing compression.

Olsen and Sperling's data.¹⁹ Swelling pressures for isolated layers of the cornea have not been reported before. Although isolated layer samples also exhibited a power law relationship, the equilibrium compressive axial stress and moduli are lower than expect based on the full thickness samples. Interactions between layers present in the intact cornea could have been lost when the layers were cut. Hence, the intact cornea would be stiffer than the effective modulus based on the isolated layers. Damage from the laser cuts, errors in axial strain calculation, and loss of macromolecules during layer isolation are also possible explanations for the low experimental values, which remain an open question.

As with all in vitro experiments on the cornea, swelling of the specimens is an important concern. Average CCT for human corneas is approximately $535 \mu\text{m}$ ²¹ so some swelling likely occurred before sample processing. Because the normal physiological CCT of the samples was not known, the axial strains calculated from pachymeter readings are an approximation with possible error due to swelling. The range of axial strain at which the tests were performed was designed to include a gap distance close to the physiological thickness of the sample. Swelling before the laser cuts is assumed to be uniform through the depth because all samples experienced only slight to moderate swelling (<20% CCT).²² Therefore, errors in axial strain calculation due to swelling for thirds from the same cornea are the same. In an effort to minimize swelling, the cornea samples were stored and refrigerated in corneal storage medium (Optisol; Bausch & Lomb) except during the laser cutting procedure and preparation immediately before testing. Additionally, the epithelium and endothelium were left intact for all samples until final preparation because removal has been shown to cause swelling of the cornea in vivo.¹⁶

Although corneal storage medium (Optisol; Bausch & Lomb) was used to prevent swelling and degradation of the corneal tissue, shear properties could change postmortem. Figure 7 shows that the anterior isolated layer samples of Donors 3 and 4 (2 weeks postmortem) are stiffer than the anterior layer samples of Donors 1 and 2 (1 week postmortem). This could be explained by changes that occurred postmortem or varying degrees of anterior lamellar interweaving between individuals.

Estimated epithelium and endothelium thicknesses were used during the calculation of laser cut depths, introducing additional sources of error in axial strain calculation. A thick epithelium would cause a thin anterior third sample while a thin or partially removed epithelium would lead to a thicker anterior third sample than desired. By a similar argument applied to the endothelium, the posterior third could be thicker or thinner than expected. Because the central third was laser cut on both sides, the only error in axial strain calculation is from swelling. This could explain why the central thirds qualitatively have less variation than the other third types (Fig. 6). Caution must be exercised when comparing measured values from different corneas at a given axial strain because samples can have different errors associated with the calculated axial strain from swelling as well as cut depths. Comparing the isolated layer samples to the full sample from Donor 2 shows that the full sample is stiffer than all the thirds for a given axial strain (Fig. 8a). However, plotting the shear moduli for the isolated layer samples as a function of axial stress and including full sample values that fall in the same axial stress range indicates that full modulus values fall in between anterior and central values for a given axial stress (Fig. 8b). In vivo measurements of certain biomechanical properties have shown little variation between properties of an individual's left and right eye.²³ Therefore, it is expected that full moduli values would fall in the range of isolated sample modulus values from the same donor. For all four donor pairs, plotting shear modulus values against axial stress satisfied this condition, while comparing with axial strain was inconsistent. Full thickness samples were tested over different calculated axial strain ranges and would be difficult to compare by axial strain. However, Figure 5 exhibits the low variability of shear modulus for a given measured axial stress.

Due to the dynamic nature of each test, every shear modulus reported is the magnitude of the complex shear modulus recorded by the rheometer. The complex shear modulus is a dynamic, viscoelastic property that includes an elastic part and a dissipative part calculated by the rheometer from the amplitudes and phase lag between the measured stress and strain curves that are sinusoidal in time. The magnitude of the complex modulus will be higher than the static shear modulus, but the complex modulus is more straightforward to measure in the laboratory. It should also be noted that the tissue at the center of the sample undergoes a smaller shear strain than the outer edge. Shear modulus calculations by the rheometer use the assumption that the modulus does not depend on strain magnitude. Preliminary studies showed this is not the case, as with most biological tissues, so a small strain amplitude was used to minimize this effect.

When calculating the shear modulus from the torsional rheometry data it is assumed that the sample is a cylinder (uniform thickness and cross-section). The corneas cut with the femtosecond laser produced three layers of uniform thickness. An uncut cornea is thinnest at its center and thickens toward the limbus. Therefore, the full thickness cornea samples were not uniform thickness and the axial strain at the center of the sample was smaller than the axial strain at the perimeter of the 6 mm button during the test. This causes additional underestimation of the axial strain calculation superimposed on the error from swelling. Future studies could use

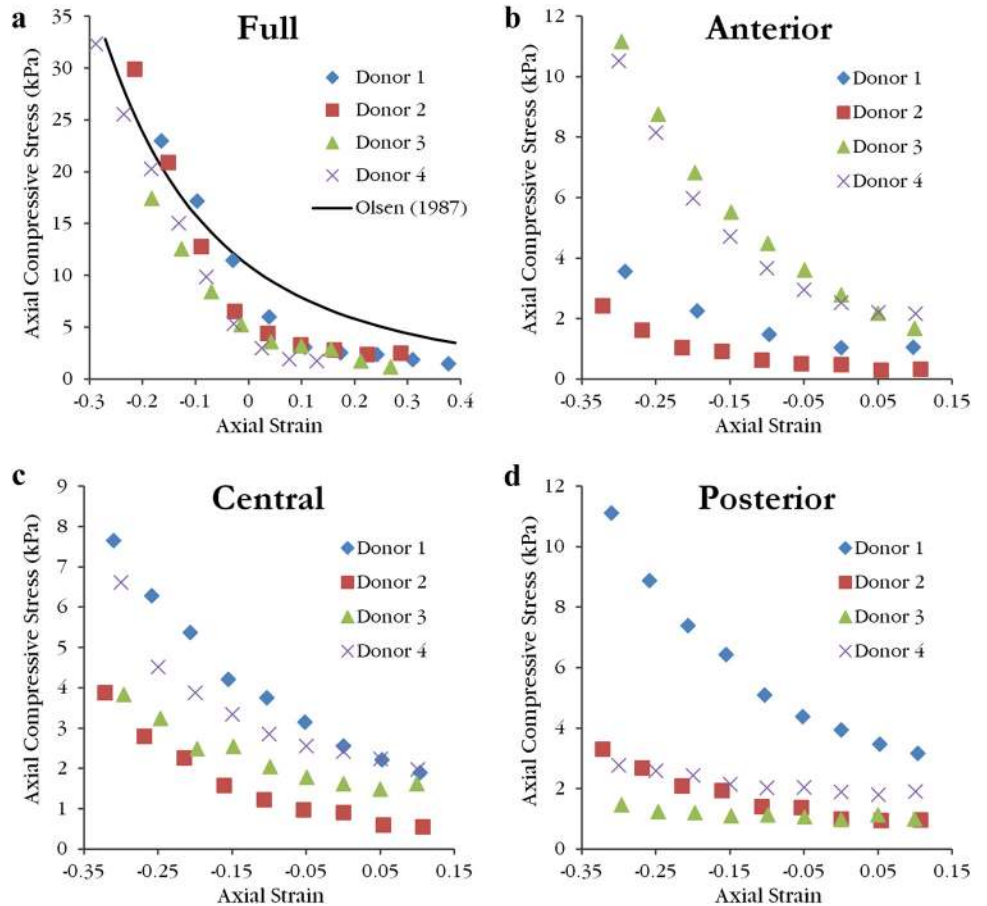


FIGURE 9. The equilibrium axial compressive stress (swelling pressure) as a function of axial strain follows a power law relationship. A power fit reported by Olsen and Sperling¹⁹ is transformed to axial strain for comparison to full thickness samples (a). Data are believed to lie below this curve as a result of the corneal storage medium (Optisol; Bausch & Lomb) bath. Swelling pressure values for anterior (b), central (c), and posterior (d) isolated layers are low compared with the full thickness sample.

the femtosecond laser to cut full thickness samples at a depth equal to the CCT to produce a uniform thickness sample that includes the entire stroma at its center. Laser cuts did not change any sample's curvature. Thus all ex vivo samples had a curvature that matched in vivo corneas. Consequently, all samples had to be flattened by the rheometer, introducing additional prestress in the tissue from bending that was neglected in the calculation of the shear properties. The in vivo cornea has a tensile prestress from intraocular pressure. Presence of an in-plane tensile prestress may produce a higher in vivo shear modulus when interwoven lamellae are present due to the nonlinear tensile behavior of collagen fibrils stretched in transverse shear deformation.

Mechanical properties of the stroma are of primary interest because the other layers are presumed to have little effect on the cornea's overall biomechanical properties. The tensile stiffness of the epithelium has been shown to be considerably lower than that of the stroma²⁴ and the thinner endothelial layer is expected to have similar properties. The epithelium

and endothelium were removed from all samples to promote more rigid gripping of the sample in the rheometer. Bowman's layer and Descemet's membrane were not removed so their mechanical contribution needs to be considered. Bowman's layer, which is approximately 10 μm thick,¹³ was present in the anterior and full samples. However, it is assumed to provide a negligible mechanical contribution because uniaxial tests of corneal strips have shown that the presence of Bowman's layer did not have significant effect.²⁵ Descemet's membrane, also approximately 10 μm thick,¹³ was present in the full samples, but may or may not have been present in the posterior samples depending on the deepest cut with the laser. The presence of Descemet's membrane has been shown to have little mechanical effect in low pressure inflation tests so its mechanical contribution to the samples was also neglected.^{26,27} Note that the mechanical contribution of these layers is ignored based on tensile data because shear property data has never been measured.

While numerous steps were taken to minimize damaging the samples during preparation, damage to lamellae and collagen fibrils is unavoidable. The raster pattern of the femtosecond laser leaves some residual tissue along the cut surface. Just before testing the layers were slowly pulled and wedged apart with forceps and a spatula, carefully dissecting the residual tissue. The tearing of tissue caused by separating the layers probably extends the damaged area of the tissue beyond the area of the laser cut. The anterior and posterior layers only had one surface that underwent the blunt dissection in contrast to both surfaces of the central third. In the posterior third, cuts followed the anterior curvature but lamellae follow the steeper posterior curvature due to the cornea becoming thicker toward the limbus; this resulted in undesired transversely cut

TABLE 3. Measured Equilibrium Compressive Modulus Values at 0% Axial Strain

Donor	Full	Anterior	Central	Posterior
1	49.0 (0.98)	3.80 (0.98)	7.65 (0.99)	10.9 (0.99)
2	42.5 (0.99)	1.80 (0.99)	3.26 (0.99)	3.11 (0.99)
3	31.7 (0.99)	11.2 (0.99)	3.82 (0.96)	0.79 (0.78)
4	31.4 (0.96)	10.1 (0.99)	6.26 (0.95)	1.90 (0.94)
Mean	38.7	6.72	5.25	4.17
SD	8.60	4.62	2.07	4.58

Data shown are kPa (R^2 value of corresponding power fit).

lamellae that were not interwoven. The damage to lamellae and fibril integrity could lead to an underestimation of the tissue's mechanical shear properties due to fewer fibrils engaged during shear deformation. This could explain why shear modulus values of uncut full samples were comparable to the anterior layer rather than falling between anterior and posterior layer as expected.

The transverse shear stiffness of an individual lamella at low shear strain is conjectured to result from the gel properties of the interfibrillar electrolyte fluid interacting with the GAG fixed charges (Pinsky PM, et al., manuscript submitted, 2012).²⁸ The transverse shear modulus resulting from this molecular mechanism is expected to be small compared with the tensile modulus resulting from the direct engagement of the collagen fibrils in tension tests.¹⁻³ Indeed, the magnitudes of the shear moduli are two to three orders lower than measured tensile moduli of the cornea.¹⁻³ This interpretation also provides an explanation for the significant dependence of shear moduli on axial compression. As the tissue is compressed, the negative charges on the GAGs between and surrounding collagen fibrils move closer together, increasing the fixed charge density which has been shown in recent work to lead to an increased shear modulus.²⁸ Electrolyte properties of the matrix could be examined by performing shear tests while varying the ionic concentration of the bath.

Acknowledgments

The authors thank Abbott Medical Optics, Inc., for help in acquisition of the human corneas, James F. Nishimuta of the Soft Tissue Biomechanics Laboratory at Stanford University, for his help with the testing protocols, and Moritz Winkler and James V. Jester's group at the University of California, Irvine, for providing the second harmonic generated image (Fig. 1).

References

1. Elsheikh A, Wang D, Brown M, Rama P, Campanelli M, Pye D. Assessment of corneal biomechanical properties and their variation with age. *Curr Eye Res.* 2007;32:11-19.
2. Elsheikh A, Brown M, Alhasso D, Rama P, Campanelli M, Garway-Heath D. Experimental assessment of corneal anisotropy. *J Refract Surg.* 2008;24:178-187.
3. Hjortdal JØ. Regional elastic performance of the human cornea. *J Biomech.* 1996;29:931-942.
4. Boyce BL, Grazier JM, Jones RE, Nguyen TD. Full-field deformation of bovine cornea under constrained inflation conditions. *Biomaterials.* 2008;29:3896-3904.
5. Christensen RM. Chapter 3.1: Transversely isotropic media. In: *Mechanics of Composite Materials*. 1st ed. New York, NY: John Wiley & Sons; 1979:74-80.
6. Pandolfi A, Fotia G, Manganiello F. Finite element simulations of laser refractive corneal surgery. *Engineering with Computers.* 2008;25:15-24.
7. Grytz R, Meschke G. A computational remodeling approach to predict the physiological architecture of the collagen fibril network in corneo-scleral shells. *Biomech Model Mechanobiol.* 2010;9:225-235.
8. Pinsky PM, van der Heide D, Chernyak D. Computational modeling of mechanical anisotropy in the cornea and sclera. *J Cataract Refract Surg.* 2005;31:136-145.
9. Nickerson CS. *Engineering the Mechanical Properties of Ocular Tissues*. Pasadena, California: California Institute of Technology; 2005. Thesis.
10. Bron AJ, Tripathi RC, Wolff E, Tripathi BJ. The cornea and sclera. In: *Wolff's Anatomy of the Eye and Orbit*. 8th ed. Chapman & Hall Medical; 1997:233-267.
11. Jester JV, Winkler M, Jester BE, Nien C, Chai D, Brown DJ. Evaluating corneal collagen organization using high-resolution nonlinear optical microscopy. *Eye Contact Lens.* 2010;36:260-264.
12. Winkler M, Chai D, Kriling S, et al. Nonlinear optical macroscopic assessment of 3-D corneal collagen organization and axial biomechanics. *Invest Ophthalmol Vis Sci.* 2011;52:8818-8827.
13. Komai Y, Ushiki T. The three-dimensional organization of collagen fibrils in the human cornea and sclera. *Invest Ophthalmol Vis Sci.* 1991;32:2244-2258.
14. Abahussin M, Hayes S, Knox Cartwright NE, et al. 3D collagen orientation study of the human cornea using X-ray diffraction and femtosecond laser technology. *Invest Ophthalmol Vis Sci.* 2009;50:5159-5164.
15. Naor J, Slomovic AR, Chipman M, Rootman DS. A randomized, double-masked clinical trial of Optisol-GS vs Chen Medium for human corneal storage. *Arch Ophthalmol.* 2002;120:1280-1285.
16. Maurice DM, Giardini AA. Swelling of the cornea in vivo after the destruction of its limiting layers. *Br J Ophthalmol.* 1951;35:791-797.
17. Reinstein DZ, Archer TJ, Gobbe M, Silverman RH, Coleman DJ. Epithelial thickness in the normal cornea: three-dimensional display with very high frequency ultrasound. *J Refract Surg.* 2008;24:571-581.
18. Svenbergh B, Bill A. Scanning electron microscopic studies of the corneal endothelium in man and monkeys. *Acta Ophthalmologica.* 1972;26:136-143.
19. Olsen T, Sperling S. The swelling pressure of the human corneal stroma as determined by a new method. *Exp Eye Res.* 1987;44:481-490.
20. Kaufman HE, Beuerman RW, Steinemann TL, Thompson HW, Varnell ED. Optisol corneal storage medium. *Arch Ophthalmol.* 1991;109:864-868.
21. Doughty MJ, Zaman ML. Human corneal thickness and its impact on intraocular pressure measures: a review and meta-analysis approach. *Surv Ophthalmol.* 2000;44:367-408.
22. Kikkawa Y, Hirayama K. Uneven swelling of the corneal stroma. *Invest Ophthalmol Vis Sci.* 1970;9:735-741.
23. Kopito R, Gaujoux T, Montard R, et al. Reproducibility of viscoelastic property and intraocular pressure measurements obtained with the Ocular Response Analyzer. *Acta Ophthalmologica.* 2011;89:225-230.
24. Elsheikh A, Alhasso D, Rama P. Assessment of the epithelium's contribution to corneal biomechanics. *Exp Eye Res.* 2008;86:445-451.
25. Seiler T, Matallana M, Sendler S, Bende T. Does Bowman's layer determine the biomechanical properties of the cornea? *Refract Corneal Surg.* 1992;8:139-142.
26. Jue B, Maurice DM. The mechanical properties of the rabbit and human cornea. *J Biomech.* 1986;19:847-853.
27. Danielsen CC. Tensile mechanical and creep properties of Descemet's membrane and lens capsule. *Exp Eye Res.* 2004;79:343-350.
28. Jin M, Grodzinsky AJ. Effect of electrostatic interactions between glycosaminoglycans on the shear stiffness of cartilage: a molecular model and experiments. *Macromolecules.* 2001;34:8330-8339.